

COMMUNICATION

Received 00th February 20xx,

Unexpected structures of the Au₁₇ gold cluster: The stars are shiningPham Vu Nhat,^{a,*} Nguyen Thanh Si,^a Vitaly G. Kiselev,^{b,c} André Fielicke,^d Hung Tan Pham^e and Minh Tho Nguyen^{f,*}

Accepted 00th February 20xx

DOI: 10.1039/x0xx00000x

The Au₁₇ gold cluster was experimentally produced in the gas phase and characterized by its vibrational spectrum recorded using far-IR multiple photon dissociation (FIR-MPD) of Au₁₇Kr. DFT and coupled-cluster theory PNO-LCCSD(T)-F12 computations reveal that, at odd with most previous reports, Au₁₇ prefers two star-like forms derived from a pentaprism added by two extra Au atoms on both top and bottom surfaces of the pentaprism, along with five other Au atoms each attached on a lateral face. A good agreement between calculated and FIR-MPD spectra indicates a predominant presence of these star-like isomers. Stabilization of a star form arises from strong orbital interactions of an Au₁₂ core with a five-Au-atom string.

Owing to their particular properties and numerous applications in devices with nanoscale dimensions,¹⁻³ such as chemical/biological sensors,⁴ in biomedical sciences⁵ and catalysis,⁶⁻⁸ gold clusters are among the most characterized transition metal nanoparticles to date.⁹ As a result of the strong relativistic effect of the element gold,¹⁰⁻¹² small pure Au_n clusters prefer a planar or quasi-planar shape, and a structural transition going from a two-dimensional (2D) to a three-dimensional (3D) configuration takes place at the sizes $n = 8 - 13$ depending on their charge states,¹³⁻¹⁶ whereas larger systems from $n = 16 - 18$ tend to exist as hollow cages.^{17,18} Some of us¹⁹ recently demonstrated a plausible coexistence of both planar and non-planar isomers of Au₁₀ at the onset of a 2D-3D structural transition of pure neutral gold clusters. Since an experimental evidence for hollow golden cages was reported for the Au₁₆⁻ and Au₁₇⁻ anions,^{17,20} several studies have been devoted to the structures and properties of these sizes. Such golden cages can also trap a foreign atom resulting in a new category of encapsulated

methods and differ greatly from each other.¹⁷⁻²⁶ While a hollow cage **17_3** (cf. Fig. 1) was predicted as a ground state,^{17,24} a distorted tetrahedral D_{2d} shape **17_6** resulting from a T_d structure of Au₁₇⁺ was also suggested.²⁵ However, a new putative ground state structure, i.e. **17_7** (Fig. 1), was more recently reported¹⁹ which is not consistent with all those proposed earlier. Recently some of us found a star-like structure (**17_2** in Fig. 1) by using the PBE functional,¹⁹ but the reliability of such a new global minimum prediction was not certain because it was based on the energies obtained with one particular DFT functional.

In view of such a discrepancy, we set out to perform a combined experimental and theoretical study to revisit the Au₁₇ structure. From extensive quantum chemical computations, we find two new structural motifs for this size that have been overlooked in the literature, and both are found to be more stable than those previously reported (Fig. S1). The calculated vibrational signatures of these new isomers are subsequently compared to the experimental far-IR spectrum recorded by IR multiple photon dissociation (IR-MPD) of the Au₁₇-Kr complex with the aim to assign the structure generated.

Quantum chemical results presented hereafter are determined using a range of DFT²⁷⁻³¹ and wavefunction theory (coupled-cluster theory)³²⁻³⁴ methods that are described in the SI file along with details on the IR-MPD experiment.

The shapes of the low-lying Au₁₇ isomers along with their symmetry point groups and relative energies are shown in Fig. 1, while their Cartesian coordinates are given in Table S1 of the SI file. Previously suggested structures given in Fig. S1 are also labeled following to those in Fig. 1. In recent calculations^{26,35} using both PW91 and BB95 functionals, the C_s **17_7** (Fig. 1) which is obtained upon removal of three corner Au atoms from the Au₂₀ tetrahedron³⁵ was reported as the global energy minimum of Au₁₇. Such an assignment is not consistent with a previous result using the TPSS functional²⁵ which yields D_{2d} **17_6** as the lowest-energy structure. The latter can be constructed by adding four Au atoms on an fcc octahedral core of Au₁₃. On the contrary, earlier calculations^{36,37} using the PBE functional predicted that the C_{2v} hollow cage **17_3** (Fig. 1) tends to dominate the Au₁₇ population, as in the Au₁₇⁻ anion.¹⁷

Almost all DFT results, and more importantly the coupled-cluster PNO-LCCSD(T)-F12 results, obtained in the present work predict both star-like cage structures **17_1** and **17_2** to be the most stable isomers of Au₁₇ (Fig. 1, Table 1). Both star forms are basically degenerate in energy and can be built from an Au₁₀ pentaprism followed by addition of two extra Au atoms on both top and bottom surfaces of the pentaprism, along with attachment of five other Au

^a Department of Chemistry, Can Tho University, Can Tho, Viet Nam

^b Novosibirsk State University, 1 Pirogova Str., 630090 Novosibirsk, Russia

^c Institute of Chemical Kinetics and Combustion SB RAS, 3 Institutskaya Str., 630090 Novosibirsk, Russia

^d Fritz-Haber-Institut der Max-Planck-Gesellschaft, Faradayweg 4-6, 14195 Berlin, Germany

^e Department of Chemistry, KU Leuven, Celestijnenlaan 200F, 3001 Leuven, Belgium

^f Institute for Computational Science and Technology (ICST), Ho Chi Minh City, Vietnam. Email: tho.nm@icst.org.vn

Electronic Supplementary Information (ESI) available. See DOI: 10.1039/x0xx00000x

golden cages, similar to endohedral fullerenes.²¹ Although several large golden cages and their derivatives were theoretically predicted,²¹⁻²³ none of them has been observed experimentally yet.

Here we will focus on the pure and neutral Au₁₇ cluster. Fig. S1 of the Supplementary Information (SI) file gives a summary of the structures previously assigned as the most stable form of Au₁₇.¹⁷⁻²⁶ They were obtained using different density functional theory (DFT)

COMMUNICATION

atoms, each on a lateral face. The main difference between them is that while two of the latter atoms form a bond in **17_1**, they are separated in **17_2**. The most striking finding is that these star-like structural motifs that have almost been overlooked in previous reports (Fig. S1, SI) could emerge as the lowest-lying isomers of Au₁₇.

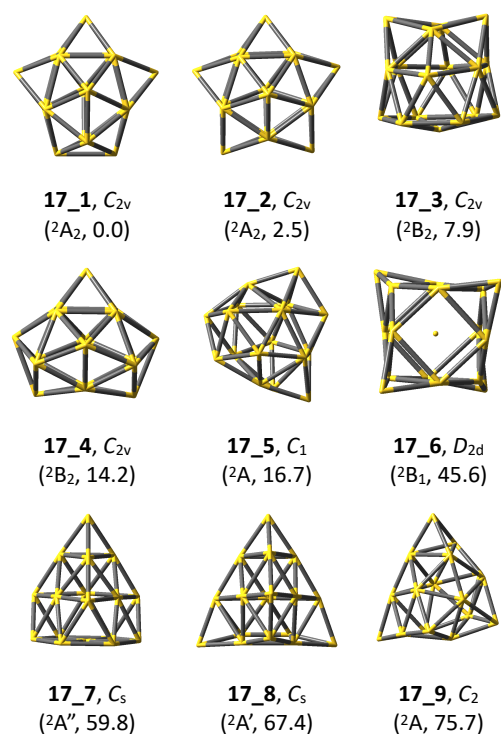


Fig. 1. Some low-lying Au₁₇ isomers along with their symmetry point groups and relative energies with respect to the lowest-lying isomer **17_1** (kJ/mol obtained from PNO-LCCSD(T)-F12b/aug-cc-pVDZ-PP + ZPE computations).

For better visualization, Fig. S2 (SI file) displays the shapes of both star forms in different perspectives. The **17_1**, **17_2**, **17_3** and **17_4** isomers displayed in Fig. 1 are slightly distorted to a C_{2v} point group, instead of adopting D_{5h} symmetry as in a regular pentaprism, due to a Jahn-Teller effect on their open-shell electronic structure. In fact, starting from a regular D_{5h} pentaprism, the doublet state of Au₁₇ has one unpaired electron occupying a degenerate e₁^{''} orbital. Such a state is not energetically stable with respect to distortion, and the system tends to undergo a geometry relaxation upon elimination of such an orbital degeneracy. More specifically, a single occupancy of one doubly degenerate orbital e₁^{''} of a higher symmetry D_{5h} structure invariably leads to a geometric change giving rise to an orbital splitting to a pair of (a₂ + b₂) orbitals in a lower symmetry C_{2v} form. The unpaired electron in the C_{2v} **17_1** occupies the a₂ SOMO (Fig. S3, SI file), thus resulting in a ²A₂ electronic state. It appears that the C_{2v} **17_3** constitutes the ²B₂ component of the splitting pair, lying ~7 kJ/mol higher in energy. Similarly, both isomers **17_2** and **17_4** seem to be formed from a splitting of another e₁^{''} orbital giving a (a₂ + b₂) pair following geometry relaxation in a different direction. The energy difference between the latter pair of isomers amounts to 10 kJ/mol (Table 1).

While both ²A₂ states keep a star-like shape, both ²B₂ components have substantially modified geometries. According to DFT results, both star-like structures **17_1** and **17_2** are strongly

competing with each other to be the ground state of Au₁₇. The TPSS functional predicts **17_2** to be slightly more favoured than **17_1** but with a tiny energy gap of 2.5 kJ/mol (Table 1). Nonetheless, calculations using another density functional may result in a different topology of the potential energy surface, as the energy ordering of isomers is known to be quite sensitive with respect to the density functional employed.^{31,38,39} In fact, while revTPSS and PBE functionals assign **17_2** as the global minimum, the PW91 and M06 predict **17_1** to be more stable, always with a small energy gap of < 4 kJ/mol. None of the functionals employed here results in **17_3**, **17_6**, **17_7** or **17_8** to be the lowest-lying isomer as previously reported (cf. Fig. S1, SI).

In this context, we perform single-point electronic energy calculations for low-lying Au₁₇ isomers using the novel local modifications of the explicitly correlated coupled-cluster theory PNO-LCCSD(T)-F12. Note that the explicitly correlated F12 procedure greatly accelerates the slow basis set convergence of conventional CCSD(T) techniques.⁴⁰ In particular, owing to more accurate pair approximations, tighter domain options and the F12 treatment of dynamic correlation, the PNO-LCCSD(T)-F12 method has been found to perform better than previous local calculations, in terms of both accuracy and cost, and yield results in reasonable agreement with the conventional CCSD(T) values.⁴¹ Very often, even a double-zeta basis set is sufficient for attaining the chemical accuracy of ± 4 kJ/mol.⁴²⁻⁴⁴ To stay on a safe side, we further compute PNO-LCCSD(T)-F12 relative energies of **17_1** - **17_6** isomers with the larger aug-cc-pVTZ-PP basis set. We find that the largest discrepancy between both DZ and TZ basis sets is < 2.5 kJ/mol (Table 1).

Table 1. Relative energies ΔE (kJ/mol) of low-lying Au₁₇ isomers computed using different methods (VnZ stands for cc-pVnZ and a for augmented)

Isomer	TPSS	revTPSS	PBE	PW91	M06	PNO-LCCSD(T)-F12b	
						VDZ-PP	aVDZ-PP aVTZ-PP
17_1	2.5	2.9	0.0	0.0	0.0	0.0	0.0
17_2	0.0	0.0	0.0	0.2	3.8	2.5	5.0
17_3	4.2	1.7	3.3	2.9	5.4	7.9	7.1
17_4	10.5	5.9	7.1	9.6	8.8	14.2	15.5
17_5	11.7	10.0	11.7	11.7	14.6	16.7	17.2
17_6	2.9	7.9	21.8	28.0	46.0	45.6	45.6
17_7	19.7	9.6	36.0	36.4	41.8	59.8	-
17_8	19.2	18.0	38.5	41.0	71.1	67.4	-
17_9	33.9	31.4	42.3	43.5	58.2	75.7	-

PNO-LCCSD(T)-F12 results again confirm that both **17_1** and **17_2** (cf. Fig. 1), being within an energy difference of ~5 kJ/mol, are the most energetically preferable isomers of Au₁₇. In agreement with PW91 and M06 predictions, **17_1** is slightly more energetically favourable whereas **17_6** becomes much less stable with a PNO-LCCSD(T)-F12 relative energy of ~46 kJ/mol. The isomers **17_3**, **17_4** and **17_5** lie also close to the global minimum **17_1** (within ~17 kJ/mol). The remaining isomers **17_7**, **17_8** and **17_9** are much less

stable, being more than 60 kJ/mol higher in energy. It is worth mentioning again that **17_6** and **17_7** were reported to be the putative global minima in previous computations (Fig. S1, SI).^{12,25,45} The present high accuracy results do not support such assignments.

In terms of free energies (ΔG), when using DFT (TPSS and revTPSS) results, **17_2** remains more stable than **17_1** by 2.1 kJ/mol at 100K, 3.3 kJ/mol at 200K, and both practically have the same free energy at 300K. Otherwise noted, the free energy ordering follows that of the corresponding enthalpy. Overall, in view of the small energy difference between both star-like isomers **17_1** and **17_2** whose ordering is interchanged with respect to the method employed, both in terms of enthalpy and free energy, we would conclude that they are basically quasi-degenerate in energy.

The high thermodynamic stability of both star-like forms can be understood with the help of orbital interactions between constituent fragments. As for a representative case, let us consider **17_2** whose electronic structure can now be analyzed by constructing orbital interactions between an inner Au₁₂ core containing a pentaprism and an outer Au₅ string. The resulting correlation diagram built up under a C_{2v} point group is illustrated in Fig. S4 (SI file) which also displays the main shell orbitals.

Such a core structure does not correspond to the lowest-lying form of Au₁₂ and lies much higher in energy than its global minimum. The five Au atoms of the outer string are located far away from each other, and do no interact with each other, and for the sake of simplicity, their 6s-MO are omitted in Fig. S4 (SI file). It is clear that the MOs of the C_{2v} Au₁₂ core are strongly stabilized upon interaction, and thereby lead to a low-energy **17_2**. A similar orbital interaction feature can also be established for the distorted star form **17_1**.

The total density of states (DOS) and some shell orbitals of **17_2** are displayed in Fig. 2. Accordingly, the 17 valence electrons of the Au₁₇ radical occupy a nearly closed electron shell of the [1S² 1P⁶ 1D⁹] configuration. It can be expected that the corresponding anion of **17_2** whose 18 valence electrons are expected to fully occupy this electron shell, is also stabilized.

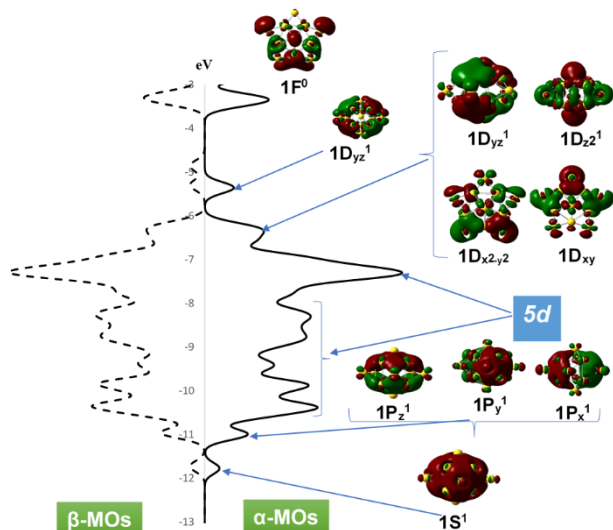


Fig. 2. Density of states (DOS) and some shell orbitals of Au₁₇ **17_2**.

We now examine the vibrational signatures of the low-lying isomers of Au₁₇ in comparison to the experimental features recorded via far-IR-MPD of Au₁₇Kr. Both the experimental and simulated IR spectra for the low-lying Au₁₇ structures are shown in

Fig. 3. Although complexation with the messenger Kr atoms may have a certain influence on the isomer distribution and appearance of IR spectra, the comparably weak interactions between krypton atoms and the neutral gold clusters is expected to induce very small effects on the IR spectra.⁴⁶

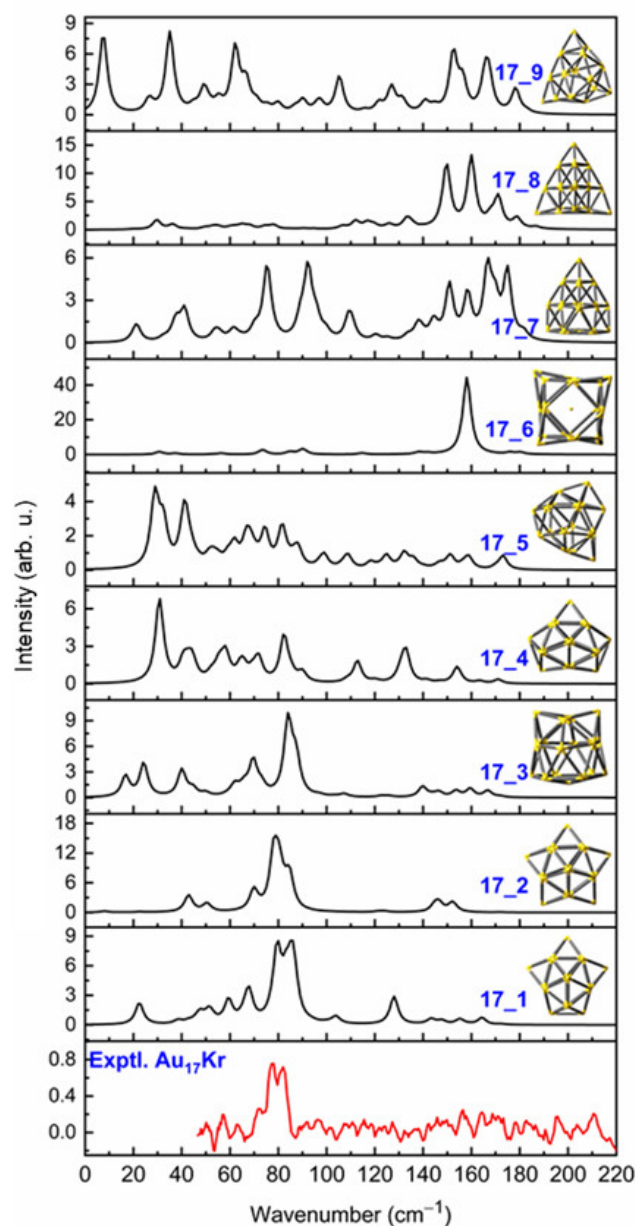


Fig. 3 Experimental FIR-MPD of Au₁₇-Kr and theoretical IR spectra of Au₁₇. Simulations are made using harmonic vibrational frequencies (without scaling) and intensities obtained by revTPSS/cc-pVDZ-PP computations.

As compared to other neutral Au_n clusters,^{47,48} the IR spectrum of Au₁₇ is rather specific with the absence of prominent bands above 100 cm⁻¹. The experimental FIR-MPD spectrum is dominated by a single broad peak centered at ~80 cm⁻¹. The predicted IR spectra of both isomers **17_1** and **17_2** are also characterized by having their most intense feature centered at 80-90 cm⁻¹, arising in each case from several overlapping absorptions. They show additional lines near 60 cm⁻¹, for which **17_1** gives a slightly better match to the experimental spectrum. Overall, both isomers **17_1** and **17_2** can well be assigned to the experimental FIR-MPD

COMMUNICATION

spectrum of Au₁₇Kr (Fig. 3). The spectrum of **17_3** exhibits a less good match to the experimental data as compared to **17_1** and **17_2**, but its contribution cannot be ruled out entirely. On the contrary, the simulated IR spectra of higher-lying isomers, i.e. from **17_4** to **17_9**, typically miss the prominent signal at ~80 cm⁻¹ but instead contain intense bands at above 100 cm⁻¹. Accordingly, they clearly do not match the experiment (Fig. 3). Because both **17_1** and **17_2** are energetically quasi-degenerate, and their IR spectra are very similar to each other, they, either just a single isomer or a mixture of both, likely contribute to the observed FIR-MPD spectrum of Au₁₇Kr. The normal coordinates of the active vibrational modes of **17_1** and **17_2** are displayed in the TOC Graphic.

In summary, by a combination of far-infrared multiple photon dissociation spectroscopy and extensive computations using DFT and wavefunction methods, structures for the neutral Au₁₇ cluster were assigned. Two new stable isomers, both having a distorted star-like shape and containing a core pentaprism capped with seven Au atoms placed outside, were identified. Formation of such golden stars is intriguing as it has never been detected before for neutral gold or other coinage metal clusters. Their vibrational signatures are characterized by stretching of bonds linked to the inner pentaprism that results in prominent peaks centered at ~80 cm⁻¹.

Experiment and Computation. Details and references are given in the Supplementary Information (SI) file.

Funding information. This work is funded by VinGroup (Vietnam) and supported by VinGroup Innovation Foundation (VinIF) under project code VinIF.2020.DA21.

Acknowledgements. AF thanks G. Meijer for his continuing support and gratefully acknowledges the Stichting voor Fundamenteel Onderzoek der Materie (FOM) in providing beam time on FELIX, the skillful assistance of the FELIX staff, and the contributions of his co-authors of Refs. 46–48 for obtaining the experimental data.

Conflicts of interest. The authors declare no competing financial interest.

References

- H. Zhang, G. Schmid and U. Hartmann, *Nano Lett.*, 2003, **3**, 305–307.
- M. C. Daniel and D. Astruc, *Chem. Rev.*, 2004, **104**, 293–346.
- P. Schwerdtfeger, *Angew. Chem. Int. Ed.*, 2003, **42**, 1892–1895.
- K. Saha, S. S. Agasti, C. Kim, X. Li and V. M. Rotello, *Chem. Rev.*, 2012, **112**, 2739–2779.
- L. A. Austin, M. A. Mackey, E. C. Dreaden and M. A. El-Sayed, *Arch. Toxicol.*, 2014, **88**, 1391–1417.
- J. H. Teles, S. Brode and M. Chabanas, *Angew. Chem. Int. Ed.*, 1998, **37**, 1415–1418.
- R. M. Veenboer, S. Dupuy, S. P. Nolan, *ACS Catal.*, 2015, **5**, 1330–1334.
- M. Rudolph and A. S. K. Hashmi, *Chem. Commun.*, 2011, **47**, 6536–6544.
- P. V. Nhat, N. T. Si, N. T. T. Tram, L. V. Duong and M. T. Nguyen, *J. Comput. Chem.*, 2020, **41**, 1748–1758.
- P. Pyykko, *Chem. Rev.*, 1988, **88**, 563–594.
- P. Schwerdtfeger, M. Dolg, W. H. E. Schwarz, G. A. Bowmaker and P. D. W. Boyd, *J. Chem. Phys.*, 1989, **91**, 1762–1774.
- B. Assadollahzadeh and P. Schwerdtfeger, *J. Chem. Phys.*, 2009, **131**, 064306.
- M. P. Johansson, I. Warnke, A. Le and F. Furche, *J. Phys. Chem. C*, 2014, **118**, 29370–29377.
- P. Pyykkö, *Chem. Rev. Soc.*, 2008, **37**, 1967–1997.
- M. Gruber, G. Heimel, L. Romaner, J.-L. Brédas and E. Zojer, *Phys. Rev. B*, 2008, **77**, 165411.
- P. V. Nhat, N. T. Si, N. T. N. Hang and M. T. Nguyen, *Phys. Chem. Chem. Phys.*, 2022, **24**, 42–47.
- S. Bulusu, X. Li, L.-S. Wang and X. C. Zeng, *Proc. Natl. Acad. Sci. USA*, 2006, **103**, 8326–8330.
- W. Huang, S. Bulusu, R. Pal, X. C. Zeng and L.-S. Wang, *ACS Nano*, 2009, **3**, 1225–1230.
- N. H. Tho, T. Q. Bui, N. T. Si, P. V. Nhat and N. T. A. Nhung, *J. Mol. Mod.*, 2022, **28**, 54–64.
- X. Xing, B. Yoon, U. Landman and J. H. Parks, *Phys. Rev. B*, 2006, **74**, 165423.
- X. Gu, M. Ji, S. Wei and X. Gong, *Phys. Rev. B*, 2004, **70**, 205401.
- L. Trombach, S. Rampino, L. S. Wang and P. Schwerdtfeger, *Chem. Eur. J.*, 2016, **22**, 8823–8834.
- Y. Gao and X. C. Zeng, *J. Am. Chem. Soc.*, 2005, **127**, 3698–3699.
- C. Tang, W. Zhu, K. Zhang, X. He and F. Zhu, *Comput. Theor. Chem.*, 2014, **1049**, 62–66.
- L. Yan, L. Cheng and J. Yang, *J. Phys. Chem. C*, 2015, **119**, 23274–23278.
- S. Li, S. Singh, J. A. Dumesic and M. Mavrikakis, *Catal. Sci. Technol.*, 2019, **9**, 2836–2848.
- J. P. Perdew and Y. Wang, *Phys. Rev. B*, 1992, **45**, 13244–13249.
- J. P. Perdew, K. Burke and M. Ernzerhof, *Phys. Rev. Lett.*, 1996, **77**, 3865.
- J. Tao, J. P. Perdew, V. N. Staroverov and G. E. Scuseria, *Phys. Rev. Lett.*, 2003, **91**, 146401.
- Y. Zhao and D. G. Truhlar, *Theor. Chem. Acc.*, 2008, **120**, 215–241.
- J. P. Perdew, A. Ruzsinszky, G. I. Csonka, L. A. Constantin and J. Sun, *Phys. Rev. Lett.*, 2009, **103**, 026403.
- H. J. Werner, P. J. Knowles, G. Knizia, F. R. Manby and M. Schütz, *Wiley Interdiscip. Rev. Comput. Mol. Sci.*, 2012, **2**, 242–253.
- Q. Ma and H.-J. Werner, *J. Chem. Theory Comput.*, 2018, **14**, 198–215.
- H.-J. Werner, P. J. Knowles, F. R. Manby, J. A. Black, K. Doll, A. Heßelmann, D. Kats, A. Köhn, T. Korona and D. A. Kreplin, *J. Chem. Phys.*, 2020, **152**, 144107.
- P. V. Nhat, N. T. Si, J. Leszczynski and M. T. Nguyen, *Chem. Phys.*, 2017, **493**, 140–148.
- S. Bulusu and X. C. Zeng, *J. Chem. Phys.*, 2006, **125**, 154303.
- A. Yang, W. Fa and J. Dong, *Phys. Lett. A*, 2010, **374**, 4506–4511.
- P. V. Nhat, N. T. Si and M. T. Nguyen, *J. Chem. Phys.*, 2020, **124**, 1289–1299.
- D. A. Götz, R. Schäfer and P. Schwerdtfeger, *J. Comput. Chem.*, 2013, **34**, 1975–1981.
- L. Kong, F. A. Bischoff and E. F. Valeev, *Chem. Rev.*, 2012, **112**, 75–107.
- Q. Ma and H.-J. Werner, *J. Chem. Theory Comput.*, 2019, **15**, 1044–1052.
- V. G. Kiselev, *Phys. Chem. Chem. Phys.*, 2015, **17**, 10283–10284.
- V. G. Kiselev and C. F. Goldsmith, *J. Phys. Chem. A*, 2019, **123**, 4883–4890.
- M. V. Gorn, N. P. Gritsan, C. F. Goldsmith and V. G. Kiselev, *J. Phys. Chem. A*, 2020, **124**, 7665–7677.
- R. R. Persaud, M. Chen and D. A. Dixon, *J. Phys. Chem. A*, 2020, **124**, 1775–1786.
- L. M. Ghiringhelli, P. Gruene, J. T. Lyon, D. M. Rayner, G. Meijer, A. Fielicke and M. Scheffler, *New J. Phys.*, 2013, **15**, 083003.
- P. Gruene, D. M. Rayner, B. Redlich, A. F. van der Meer, J. T. Lyon, G. Meijer and A. Fielicke, *Science*, 2008, **321**, 674–676.
- B. R. Goldsmith, J. Florian, J.-X. Liu, P. Gruene, J. T. Lyon, D. M. Rayner, A. Fielicke, M. Scheffler and L. M. Ghiringhelli, *Phys. Rev. Mater.*, 2019, **3**, 016002.